Bearing fault diagnosis employing Gabor and augmented architecture of convolutional neural network

N. Fathiah Waziralilah[1]*, Aminudin Abu[1], M. H. Lim[2], Lee Kee Quen[1], Ahmed Elfakharany[3]

[1]Intelligent Dynamics System, Malaysia Japan International Institute of Technology, Universiti Teknologi Malaysia, Jalan Sultan Yahya Petra, 54100 Kuala Lumpur, Malaysia
*Email: tiah14@gmail.com
Phone: +60322031351
[2]Institute of Noise and Vibration, Faculty of Mechanical Engineering, Universiti Teknologi Malaysia, Jalan Sultan Yahya Petra, 54100 Kuala Lumpur, Malaysia
[3] CAIRO, Universiti Teknologi Malaysia, Jalan Sultan Yahya Petra, 54100 Kuala Lumpur, Malaysia

ABSTRACT

The vast impact on machinery that is rooted by bearing degradation thus pinpointing bearing fault diagnosis as indubitably very crucial. The research is innovated to diagnose the fault in bearing by implementing deep learning approach which is Convolutional Neural Network (CNN) that has superiority over image processing and pattern recognition. A novel model comprises of Gabor transform and augmented CNN is proposed whereby Gabor transform is utilized in representing the raw vibration signals into its 2D image representation, Gabor spectrogram. The augmented CNN is formed by alteration of the present CNN architecture. Gabor spectrogram are fed into the augmented CNN for training and testing in diagnosing the faults of bearings. To date, the method combination for bearing fault diagnosis application is inadequate. Plus, the usage of Gabor transform in mechanical area especially in bearing fault diagnosis is meagrely reported. At the end of the research, it is perceived that the proposed model comprises of Gabor transform and augmented CNN can diagnose the bearing faults with eminent accuracy and perform better than when CNN is fed with raw signals.

Keywords: bearing fault diagnosis; convolutional neural network; deep learning; Gabor spectrogram; image processing.

INTRODUCTION

For decades, bearing has represented as main source of faults in equipment. In Georgoulas [1] research, it is discerned that bearing can constitute 44% of the total number of faults in some devices. As bearing degradation could yield immense impact on the performance, stability and life span of the rotating machinery [2], ergo bearing fault diagnosis is indisputably imperative. Therefore, the past decades have manifested an increasingly number of comprehensive researches in bearing fault diagnosis [3].

In this research, convolutional neural network (CNN) method approach would be deployed in diagnosing rolling bearing faults. The CNN is selected attributable to its significant ability in image processing and pattern recognition. For instance, CNN in image processing and pattern recognition is already practiced in medical field [4], face recognition [5] and language processing [6]. Nonetheless, the application of CNN for image processing and pattern recognition in fault diagnosis is still inadequate. Formerly, in fault diagnosis, CNN is only applied to automatically select features from the generated vibration signal which is in one-dimensional input of time domain. Vibration signals provide a useful information regarding the state of the assets either equipment or structure [7–9]. Although the direct usage of CNN on the generated vibration signals is widely used and step-less, only time data could be extracted whereas the significant spatial data of the signals which in this case is the sequence of frequency as stated by Janssens et al. [10] could not be interpreted. Therefore, the utilization of CNN in processing input image of bearing raw signal is immensely essential. Ince [11] claimed that he was among the pioneer that employ 1D CNN that functioned as feature extractor and classifier to detect fault in mechanical system. As the proposed method could learn directly from raw data and any transformation or post processing are not required, low computational cost could be achieved. Author also managed to achieve more than 97% accuracy of classification process with less dependence to experts and signal pre-processing time.

Then, Jing [12] has added SoftMax regression layer as the last layer to increase accuracy and fast computation. CNN was used to learn feature directly from raw data and produce the diagnosed result. He uncovered that CNN outperforms the traditional machine learning such as support vector machine (SVM) in feature extraction and classification as the accuracy escalates in amount of 10 percent. Author also scrutinized the effectiveness of CNN in learning from different data types and made a hypothesis that CNN would work better with 2D than 1D data

The hypothesis in [12] is then validated by Zhang [13] study where he noticed the 2% increase in diagnosing accuracy when signal image is being fed into CNN compared to when using raw data as input. A study of employing CNN with image representation of vibration signal as the input also presented by Verstraete [14]. In his study, he probed the most effective form of image representation of vibration signal and found that scalogram is the best in representing signal compared to Hilbert images and spectrogram. Despite the interest in utilization of method to represent the bearing raw signal into its 2D form, Gabor transform has been overlooked. The reputation of Gabor transform is well-known in other area such as medical diagnosis [15], sleep analysis [16], seismic analysis [17], audio analysis [18], power quality analysis [19] and bearing fault detection [20]. Nevertheless, the application of Gabor transform in mechanical diagnosis area especially in bearing fault diagnosis is extremely scant. Hence, it gain the interest of the authors to deepen the comprehension in this matter. In addition, combination of Gabor and CNN is meagerly reported in bearing fault diagnosis.

The objective of the study is to determine the model performance of the proposed combination method. At the same time, the type of input of CNN is investigated whether 2D images or raw signal yield the best accuracy of the proposed model.

METHODOLOGY

Proposed Bearing Fault Diagnosis Model
The proposed model is established with combination of Discrete Gabor transform (DGT) and CNN. DGT will be applied onto the raw signal to generate the 2D image representation of bearing signal. The 2D data is then fed into CNN for bearing fault classification. The framework of the proposed model is illustrated as in Figure 1.
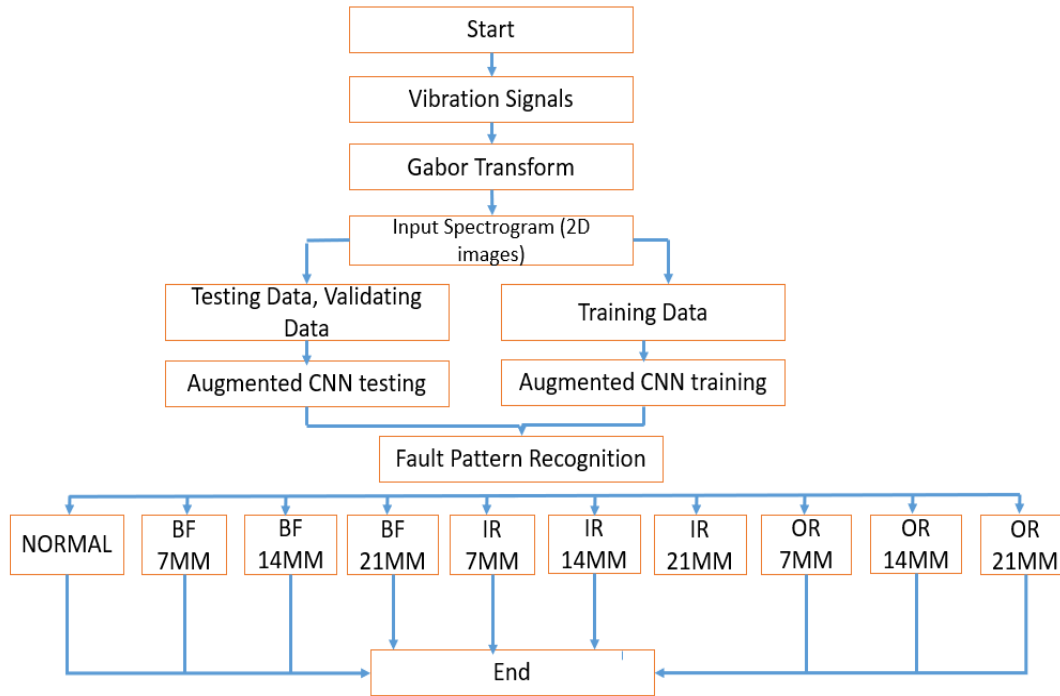

Figure 1. The Overall Framework of Proposed Model.

Gabor Transform
Gabor transform is a special case of the short-time Fourier transform (STFT). STFT is chosen as it was more applicable for real-time processing of signals due to its short processing time. The successive output of STFTs can provide a time-frequency representation of the signal [21] and useful information from the vibration signals [22]. Here, Discrete Gabor Transform (DGT) computes the Gabor coefficients of the input signal and1 generate output of matrix. The spectrogram is then returning the image to be displayed as a matrix. The finite DGT of a signal f of length L is defined in Equation 1.

$$c(m+1, n+1) = \sum_{l=0}^{L-1} f(l+1) \overline{g(l-an+1)} \, e^{-2\pi i l m/M} \tag{1}$$

where m=0, M-1 and n=0,..N-1 and *l-an* is the computed modulo L, N=L/a whereby the input parameters consist of: *f* is the input signal, *g* is the window function, *a* is the length of time shift, M is number of channels, L is the length of transform to do. The output parameters are c which is M x N array.

Figure 2 shows the sample data of raw signal data while Figure 3 shows its 2D representation which is the Gabor Spectrogram. The Gabor Spectrogram is 2D images of the raw signal and it contains the time data, frequency data and the spatial data of the raw signal. In this study, the Gabor Spectrogram would be the input fed into the CNN. Gabor Spectrogram is hypothesised in rising to a more accurate analysis compared to the raw signal.
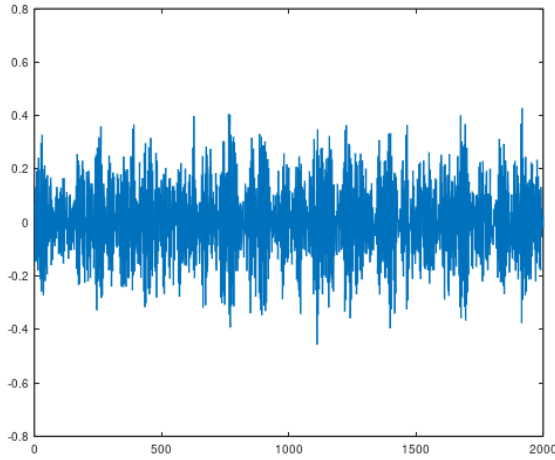

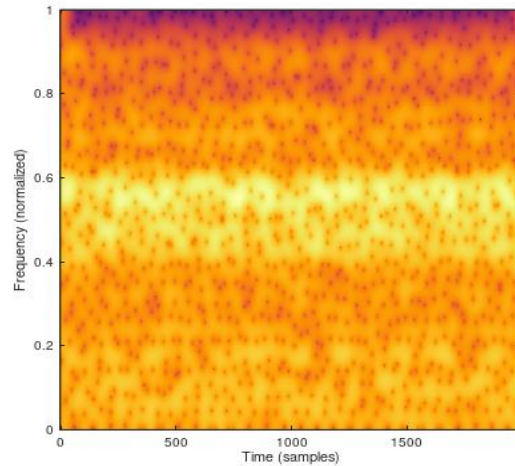
Figure 2. Raw Signal of Ball Fault 7mm 1hp

Figure 3. Gabor Spectrogram of Ball Fault 7mm 1hp.

Proposed Convolutional Neural Network
In this research, the proposed architecture of CNN implemented is shown as in Figure 4. The proposed architecture consists of two stages. Data normalization is implemented to all the training and testing of 2D data. This is to ensure the CNN model to converge faster. The first stage is made up of two stacked of Convolutional Layer with 16 feature maps which are then activated by Rectified Linear Unit (ReLU) layer and there are regularises $l2$ =0.0001 followed by normalization layer and a max pooling layer. At the end of pooling layer, is a dropout layer of 0.25. After a dropout process, the next feature maps size should be bigger due to data reduction occurs in dropout layer.

The second stage is made up similarly like the first stage but with bigger feature maps on the convolutional layer which is 32. The filter used for convolutional layer is (3x3) filter, small number of filters is used for fast computation. Then, all the filter used in pooling layer is (2x2). The output is then flattened so they become a single column output to be fed into the fully connected layers. There are two fully connected layers with feature maps of 64 and then followed by a dropout layer of 0.5.

SoftMax layer is then placed at the end of the network to classify the output into 10 classes. The SoftMax function will normalize the output in range from 0 to 1. In this study, the one-hot encoding is implemented so the output will transform into binary form. Therefore, SoftMax and one-hot encoding are deployed respectively to CNN output layer. Lastly, the predicted classification output would be the true labelled output. Cross-entropy between the estimated SoftMax output probability distribution and the target class probability distribution are the loss function applied in the proposed model. Let $p(x)$ represents the target

distribution and *q(x)* represents estimated distribution, subsequently the cross-entropy between *p(x)* and *q(x)* is depicted in Equation (2)

$$H(p, q) = -\sum_x p(x) \log q(x) \tag{2}$$

The output is obtained from summation over 10 classes and the loss represent how far is the prediction form the true distribution. To lessen the loss function, the Adam stochastic optimization algorithm is applied to train the proposed model.
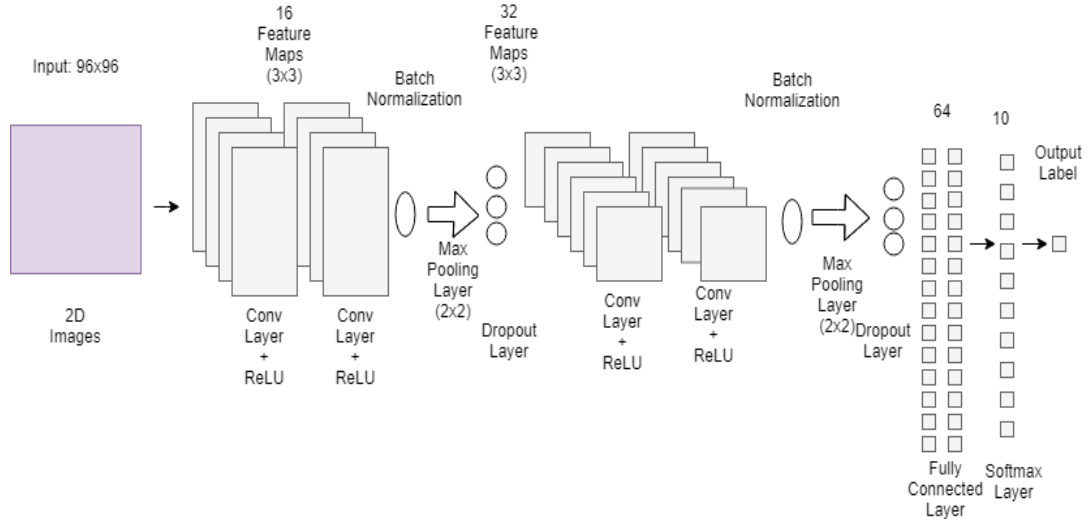

Figure 4. Proposed CNN Architecture

Convolutional neural network

CNN is particularly designed to attend to two-dimensional input data [23]. It is a multi-stage neural network which is composed of some filter stages and one classification stage as stated by W. Lu *et al.* [24]. The filter stage is designed to extract features from the inputs. The proposed architecture of filter stage contains five types of layer which are convolutional layer, activation layer, batch normalization layer, pooling layer and dropout layer. The classification stage is composed of two fully connected layers for classification. The function of each type of layer is defined as follows:

Convolutional layer

The convolutional layer convolves the input local regions with filter kernel then generates the stack of filtered output. K_i^l and b_i^l are used to denote the weights and bias of the i-th filter kernel in layer *l*, respectively, and use $X^l(j)$ to denote the *j*-th local region in layer *l*. The convolutional process is described as in Equation (3):

$$y_i^{l+1}(j) = K_i^l * X^l(j) + b_i^l \tag{3}$$

where the notation * computes the elementary wise multiplication of the kernel and the local regions, and $y_i^{l+1}(j)$ denotes the input of the *j*-th neuron in frame *i* of layer *l+1*.

Activation layer: ReLU layer

The activation layer employed in this proposed architecture Rectified Linear Unit (ReLU) layer. The layer is applied after the convolutional process. Generally, it works by replacing

all the negative pixel values in the feature maps by zero. The process is defined in Equation (4). This layer is used to accelerate the convergence of the CNN.

$$a_i^{l+1}(j) = f\left(y_i^{l+1}(j)\right) = \max\{0, y_i^{l+1}(j)\} \tag{4}$$

where $a_i^{l+1}(j)$ is the activation of the output from the convolution operation which is $y_i^{l+1}(j)$.

Batch normalization layer
In this research, the batch normalization layer is deployed after the activation layer which is different than most of previous architecture [2] that deploy the layer before the activation layer and right after the convolutional layer. This layer is designed to reduce the shift of internal covariance and accelerate the training process of deep neural network.   The transformation of BN layer is described as in Equation (5) and (6):

$$\widehat{y}^{l(i,j)} = \frac{y^{l(i,j)} - \mu_\beta}{\sqrt{(\sigma_\beta^2 + \epsilon)}} \tag{5}$$

$$z^{l(i,j)} = \gamma^{l(i)}\widehat{y}^{l(i,j)} + \beta^{l(i)} \tag{6}$$

where $z^{l(i,j)}$ is the output of one neuron response, $\mu_\beta = E[y^{l(i,j)}], \sigma_\beta^2 = Var[y^{l(i,j)}], \epsilon$ is a small constant added for numerical stability, $\gamma^{l(i)}$ and $\beta^{l(i)}$ are the scale and shift parameters to be learned, respectively.

Pooling layer: Max pooling layer
The aim of pooling layers aim is to gradually reduce the dimensionality of the representation, hence further diminish the number of parameters and the computational intricacy of the model [25]. The max-pooling transformation is portrayed as in Equation (7):

$$P_i^{l+1}(j) = \max_{\substack{(j-1)W+1<t_x\leq jW \\ (j-1)H+1<t_y\leq jH}}\{Q_i^l(t)\} \tag{7}$$

W and *H* are the width and height of the pooling region respectively, Q(t) denotes the value of *t*-th neuron in the *i*-th frame of layer *l*, $P_i^{l+1}(j)$ denotes the corresponding value of the neuron in layer $l + 1$ of the pooling operation.

Fully connected layer
The output from the convolutional and pooling layers represent high-level features of the input image. In the output layer, the SoftMax function is employed to transform the logits of the ten neurons to conform the form of probability distribution for the ten different bearing health conditions. The SoftMax function is described in Equation (8):

$$f(z_j) = \frac{e^{z_j}}{\sum_k^{10} e^{z_k}} \tag{8}$$

where z_j denotes the logits of the *j*-th output neuron.

Data Description
In this study, the data used to evaluate the proposed method is downloaded from the Case Western Reserve University Bearing Data Center. There are four types of bearing data included in the study, namely normal, inner race fault (IR), outer race fault (OR) and ball fault (B). The single point fault datasets were further designated by the fault size which are 0.007 inch, 0.014 inch and 0.021 inch. In this paper, there is only two datasets used that are

varied by the motor load condition of 0 to 1 hp which are Dataset A and Dataset B respectively. In every dataset, the total of fault conditions for each load is nine and in addition of one healthy data. For each dataset, there are 10000 of data that are split into training data, testing data and validation data into ratio of 70:15:15. Each data contains 2000 points of vibration signals which has sampling frequency of 12kHz. Altogether, the total of training samples, testing samples and validation samples that are randomly selected are 14000, 3000 and 3000 respectively. All the elaborated data is shown as in Table 1.

Table 1. Description of Rolling Bearing Datasets.

Fault Location	Data Type	None	Ball			Inner Race			Outer Race		
Fault Type		0	1	2	3	4	5	6	7	8	9
Fault Diameter (inch)		0	0.007	0.014	0.021	0.007	0.014	0.021	0.007	0.014	0.021
Dataset A (0 hp)	Train	700	700	700	700	700	700	700	700	700	700
	Test	150	150	150	150	150	150	150	150	150	150
	Val	150	150	150	150	150	150	150	150	150	150
Dataset B (1 hp)	Train	700	700	700	700	700	700	700	700	700	700
	Test	150	150	150	150	150	150	150	150	150	150
	Val	150	150	150	150	150	150	150	150	150	150

Comparison Study

The proposed model will be compared with the exact same CNN architecture but with different input which is the raw vibration signal that only contain time data. This juxtaposition is made to manifest the significance of extracted spatial data in CNN application in fault diagnosis.

Quantification of Model Performance

In order to quantify the performance of different fault diagnosis model, four error measurements metrics will be calculated which are accuracy, precision, recall and F-measure. The formula of the error measurements is as shown in Table 2.

Table 2. Error Calculation Formula [10,26]

Accuracy	$\dfrac{[TP] + [TN]}{[TP] + [FP] + [FN] + [TN]} \times 100$
Precision	$\dfrac{[TP]}{[TP] + [FP]} \times 100$
Recall	$\dfrac{[TP]}{[TP] + [FN]} \times 100$
F-measure	$2\dfrac{[Precision \times Recall]}{[Precision + Recall]}$

[TP] = number of true positive classifications
[TN]= number of true negative classifications
[FP]= number of false positive classifications
[FN]= number of false negative classifications

RESULTS & DISCUSSION

From this study, the proposed novel model is envisaged to be more accurate in classifying bearing condition as this model can learn from the spatial data that most of the previous developed model could not learn from due to the learnt data is only consist of time data. Plus, the close representation of bearing raw signal into its 2D images using Gabor Spectrogram would contribute into the accuracy portrayed by the synthesized novel model. The performance of the synthesized model for every dataset is defined with the accuracy, precision, recall and F-measure. The results are shown as in Table 3.

Table 3. Score of Model (Gabor + Augmented CNN)

Metrics	Accuracy	Precision	Recall	F-measure
Dataset A	1.0	1.0	1.0	1.0
Dataset B	1.0	1.0	1.0	1.0

From the Table 3, all the dataset shown 100% accuracy and all other metrics to quantify the performance of the model also shown a promising result whereby all have 1.00 of score. It is proven that when CNN is fed with Gabor Spectrogram in visualizing the raw signal, CNN can learn the features illustrated in the image very well. This is because Gabor functions is discovered to be able to model the simple cells in the visual cortex of mammalian brains [27], hence, image analysis by the Gabor transform is similar to perception in the human visual system [28]. Thus, the bearing signal can be illustrated well by the Gabor spectrogram. Besides, the modification made on the CNN architecture accelerated the deep neural network

training process, so the augmented CNN is able to classify the Gabor spectrogram accurately into their respective classes.

The model training and testing accuracy and loss are illustrated in Figure 5 and Figure 6 respectively. The figures obtained representing Dataset B model training and testing.
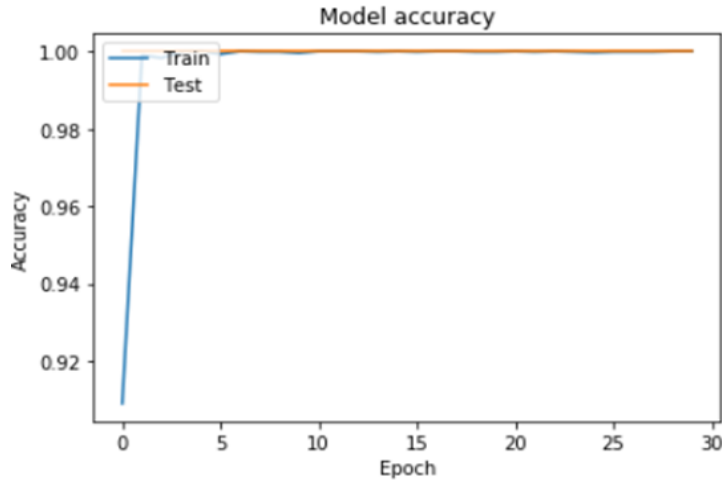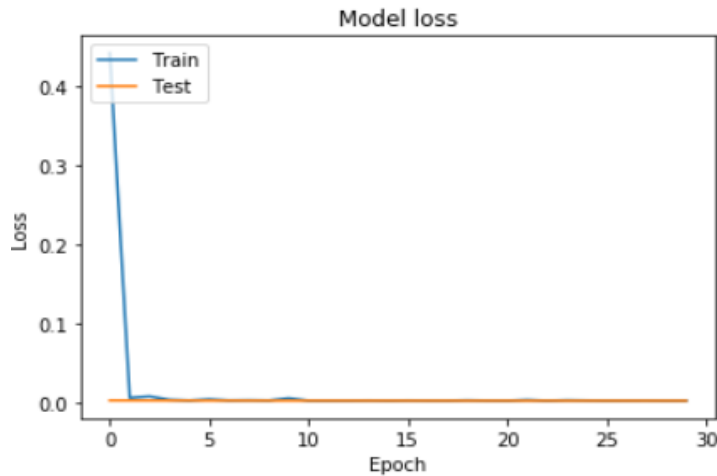

Figure 5. Proposed Model Accuracy (Dataset B)

Figure 6. Proposed Model Loss (Dataset B)

From Figure 5 and 6, the model training and testing process after 30 epochs are well performed. In every epoch, an entire dataset is passed both forward and backward through the CNN or in other words, CNN will learn all the presentation of the entire training dataset B. The total of training dataset B is 7000 which is the 70% of the total dataset B and this ratio is designated so the model is trained with big amount of training data. Additionally, the deep neural network model will perform better if the amount of training data is big [29]. The model is also generalized enough which means after the model is trained with training data, model can make an accurate prediction when fed with new testing data.

From Figure 5 and 6, it is also perceived that only a small number of epochs is taken and even at 2nd epochs, the model starts to converge. Overfitting model is indicated by the

large gap between training and testing accuracy and loss [30]. As shown in the Figure 5 and 6, the training and testing process of accuracy and loss are almost similar with each other therefore the model is proven to be not overfitting. This implies the model is reliable enough for diagnosis process of the bearing. The model loss is 0.00666 which is minute, and the model accuracy is 1.00 or 100% thus reflecting the model has been validated to work well. The confusion matrix of model from Dataset A and Dataset B are shown as in Figure 7 and Figure 8 correspondingly.
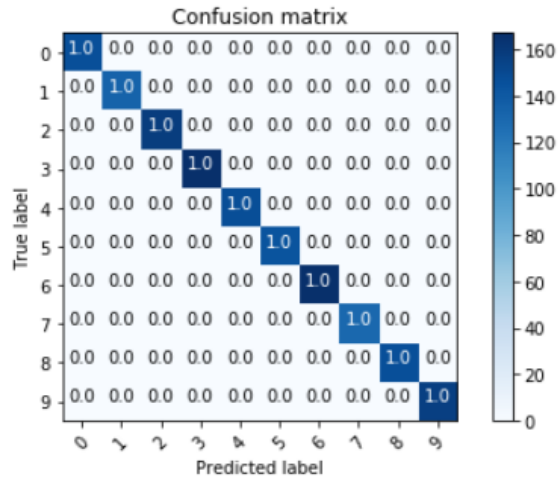

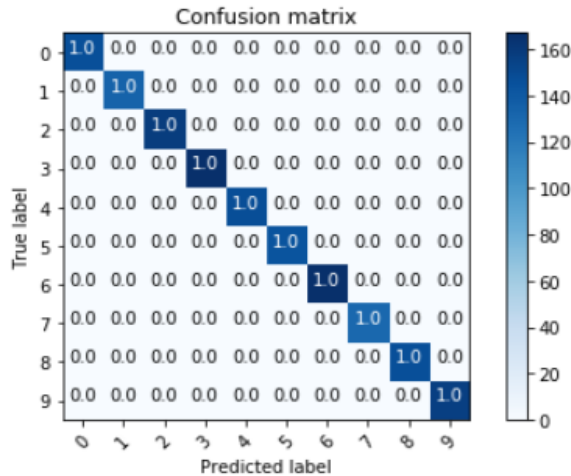Figure 7. Confusion Matrix of Dataset A (Gabor)

Figure 8. Confusion Matrix of Dataset B (Gabor)

Each row of the confusion matrix represents the instances of the true label of the class and each column represents the instances of a predicted label of the class. Based on the confusion matrix illustrated in figures above, it is perceived that all the bearing faults were classified correctly into their classes. There is no misclass of the bearing condition.

Table 4. Comparison of Method for Dataset A

Input Fed To CNN	Number of Parameter	Accuracy [%]	Loss
Gabor Spectrogram (2D)	1104826	100	0.00660
Gabor Spectrogram(2D)	4416874	100	0.13216
Raw Signal (1D)	1030490	99.47	0.02747
Raw Signal (1D)	4118730	99.80	0.03101

Table 5. Comparison of Method for Dataset B

Input Fed To CNN	Number of Parameter	Accuracy [%]	Loss
Gabor Spectrogram (2D)	1104826	100	0.00666
Gabor Spectrogram (2D)	4416874	100	0.01306
Raw Signal (1D)	1030490	99.60	0.03046
Raw Signal (1D)	4118730	100	0.01382

Table 4 and Table 5 show the comparison of performance for different input that fed into CNN for Dataset A and Dataset B respectively. Model of CNN when fed with Gabor Spectrogram can easily reached 100% accuracy with only small network of CNN. Even with a bigger network that involves more parameters, the model still can obtain high accuracy. In determination of the best CNN model from two model that has same accuracy, the number of parameters involves is investigated. When two model has same accuracy, the best model would be the model with less parameter involved. This is because, few parameters involved means the computation is cheaper and faster compared to a model with more parameters. However, when CNN is fed with raw signal which is in 1D form, the model only achieves 99.60% of accuracy. Even though, the accuracy is quite high and considering the CNN could learn directly from raw data making raw data is a good input to fed into the CNN, but the testing process is not smooth enough. The accuracy and loss of the raw model training and testing process are shown as in Figure 9 and Figure 10. The figures from Dataset B are taken as the example.
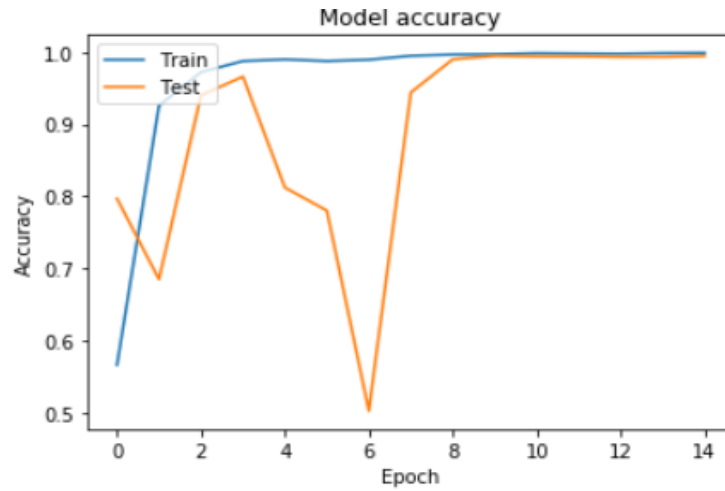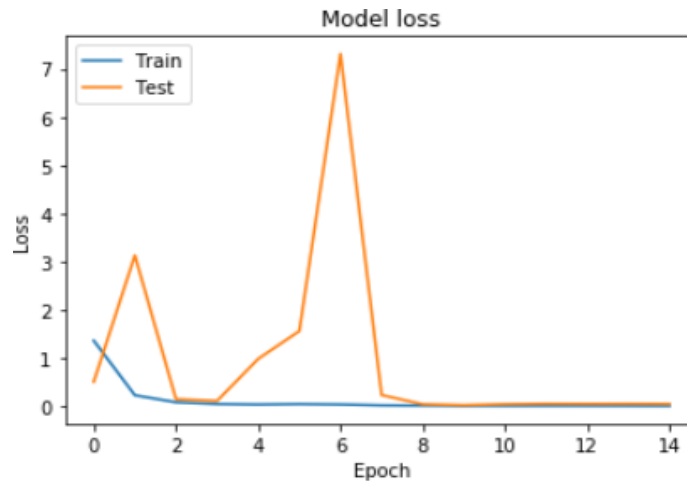
Figure 9. Raw Model Accuracy (Dataset B)

Figure 10. Raw Model Loss (Dataset B)

From Figure 9 and 10, the model testing is apparent to be quite bad. From the beginning of the epoch until the 8th epoch, the testing process has not been converged. The model testing should be similar to model training and this show the model is not performing well enough despite the high accuracy obtained which is 99.60%. The training and testing process of the raw model are not well than the Gabor training and testing process which is smoother and almost similar. Therefore, Gabor transform would be the best option as an input to CNN compared to the raw signal.

CONCLUSION

From this study, it is concluded that classification of faults is dealt better by CNN when the input is 2D image of bearing signal instead of raw signal data. This is because 2D image consists of more data such as the spatial data which in this case is the sequence of the frequency, the frequency and time data. The proposed model also shown an outstanding performance with accuracy of 100% regardless of small number of parameters involved.

ACKNOWLEDGEMENT

REFERENCES

[1]   Georgoulas G, Loutas T, Stylios CD, Kostopoulos V. Bearing fault detection based on hybrid ensemble detector and empirical mode decomposition. Mech Syst Signal Process 2013;41:510–25.

[2]   Zhang W, Li C, Peng G, Chen Y, Zhang Z. A deep convolutional neural network with new training methods for bearing fault diagnosis under noisy environment and different working load. Mech Syst Signal Process 2018;100:439–53.

[3]   Hui KH, Lim MH, Leong MS, Al-Obaidi SM. Dempster-Shafer evidence theory for multi-bearing faults diagnosis. Eng Appl Artif Intell 2017;57:160–70.

[4]   Kayalibay B, Jensen G, van der Smagt P. CNN-based Segmentation of Medical Imaging Data. 2017.

[5]   Haidong S, Hongkai J, Xingqiu L, Shuaipeng W. Intelligent fault diagnosis of rolling bearing using deep wavelet auto-encoder with extreme learning machine. Knowledge-Based Syst 2017.

[6]   Goldberg Y. A Primer on Neural Network Models for Natural Language Processing. ArXiv Prepr ArXiv151000726 2015:1–76.

[7]   Rahman N, Alam MN, Junaid M. Active vibration control of composite shallow shells: An integrated approach. J Mech Eng Sci 2018;12:3354–69.

[8]   Hussin WNW, Harun FN, Mohd MH, Rahman MAA. Analytical modelling prediction by using wake oscillator model for vortex-induced vibrations. J Mech Eng Sci 2018;11:3116–28.

[9]   N. Mohamad, J. Yaakub, H.E. Ab Maulod, A.R. Jeefferie, M.Y. Yuhazri, K. T. Lau, Q. Ahsan MIS and RO. Vibrational damping behaviors of graphene nanoplatelets reinforced NR/EPDM nanocomposites. J Mech Eng Sci 2017;11:3274–87.

[10]   Janssens O, Slavkovikj V, Vervisch B, Stockman K, Loccufier M, Verstockt S, et al. Convolutional Neural Network Based Fault Detection for Rotating Machinery. J Sound Vib 2016;377:331–45.

[11]   Ince T, Kiranyaz S, Eren L, Askar M, Gabbouj M. Real-Time Motor Fault Detection by 1-D Convolutional Neural Networks. IEEE Trans Ind Electron 2016;63:7067–75.

[12]   Jing L, Zhao M, Li P, Xu X. A convolutional neural network based feature learning and fault diagnosis method for the condition monitoring of gearbox. Measurement 2017;111:1–10.

[13]   Zhang L, Xiong G, Liu H, Zou H, Guo W. Bearing fault diagnosis using multi-scale entropy and adaptive neuro-fuzzy inference. Expert Syst Appl 2010;37:6077–85.

[14] Verstraete D, Ferrada A, Droguett EL, Meruane V, Modarres M, Meruane V, et al. Deep Learning Enabled Fault Diagnosis Using Time-Frequency Image Analysis of Rolling Element Bearings. Shock Vib 2017;2017:1–17.

[15] Garg N, Babbar N. Feature Extraction of Wrist Pulse Signals using Gabor Spectrogram. Indian J Sci Technol Vol 9, Issue 47, December 2016 2016.

[16] Huon L-K, Lo M-T, Chang Y-C, Chen Y-J, Wang P-C. Evaluation of Upper Airway in Obstructive Sleep Apnea: Synchronized Imaging and Acoustic Analyses. Otolaryngol Neck Surg 2013.

[17] Tian L, Peng Z, Zhang Q. Deconvolution-fractional Gabor spectrogram for seismic signal spectral decomposition. Shiyou Diqiu Wuli Kantan/Oil Geophys Prospect 2015.

[18] Gu Y, Postma E, Lin HX, Van Den Herik J. Speech emotion recognition using voiced segment selection algorithm. Front. Artif. Intell. Appl., 2016.

[19] Abdullah AR, Sha'ameri AZ, Saad NM. Power quality analysis using spectrogram and gabor transformation. 2007 Asia-Pacific Conf. Appl. Electromagn. Proceedings, APACE2007, 2007.

[20] Rosero J, Cusidó J, Garcia Espinosa A, Ortega JA, Romeral L. Broken bearings fault detection for a permanent magnet synchronous motor under non-constant working conditions by means of a joint time frequency analysis. IEEE Int. Symp. Ind. Electron., 2007.

[21] Kiymik MK, Güler I, Dizibüyük A, Akin M. Comparison of STFT and wavelet transform methods in determining epileptic seizure activity in EEG signals for real-time application. Comput Biol Med 2005;35:603–16.

[22] Isham MF, Leong MS, Hee LM, Ahmad ZAB. Iterative variational mode decomposition and extreme learning machine for gearbox diagnosis based on vibration signals. J Mech Eng Sci 2019;13.

[23] Al-Saffar AAM, Tao H, Talab MA. Review of deep convolution neural network in image classification. 2017 Int. Conf. Radar, Antenna, Microwave, Electron. Telecommun., 2017, p. 26–31.

[24] Lu W, Liang B, Cheng Y, Meng D, Yang J, Zhang T. Deep Model Based Domain Adaptation for Fault Diagnosis. IEEE Trans Ind Electron 2017;64:2296–305.

[25] Shea KO, Nash R. An Introduction to Convolutional Neural Networks. ArXiv 2015:1–8.

[26] Shao H, Jiang H, Zhang H, Duan W, Liang T, Wu S. Rolling bearing fault feature learning using improved convolutional deep belief network with compressed sensing. Mech Syst Signal Process 2018;100:743–65.

[27] Daugman JG. Complete Discrete 2-D Gabor Transforms by Neural Networks for Image Analysis and Compression. IEEE Trans Acoust 1988;36:1169–79.

[28] Lee TS. Image representation using 2d gabor wavelets. IEEE Trans Pattern Anal Mach Intell 1996;18:959–71.

[29] Zhu X, Vondrick C, Fowlkes CC, Ramanan D. Do We Need More Training Data ? 2011.

[30] Koroteev M. Machine Learning Models Overfitting and Generalization in Very Big Datasets 2018;10:75–8.